



Stability of the modulator in a plasma-modulated plasma acceleratorJ. J. van de Wetering ^{1,*}, S. M. Hooker ¹ and R. Walczak ^{1,2}¹*John Adams Institute for Accelerator Science and Department of Physics, University of Oxford, Denys Wilkinson Building, Keble Road, Oxford OX1 3RH, United Kingdom*²*Somerville College, Woodstock Road, Oxford OX2 6HD, United Kingdom*

(Received 27 March 2023; accepted 19 May 2023; published 19 July 2023)

We explore the regime of operation of the modulator stage of a recently proposed laser-plasma accelerator scheme [Phys. Rev. Lett. **127**, 184801 (2021)], dubbed the plasma-modulated plasma accelerator (P-MoPA). The P-MoPA scheme offers a potential route to high-repetition-rate, GeV-scale plasma accelerators driven by picosecond-duration laser pulses from, for example, kilohertz thin-disk lasers. The first stage of the P-MoPA scheme is a plasma modulator in which a long, high-energy “drive” pulse is spectrally modulated by copropagating in a plasma channel with the low-amplitude plasma wave driven by a short, low-energy “seed” pulse. The spectrally modulated drive pulse is converted to a train of short pulses, by introducing dispersion, which can resonantly drive a large wakefield in a subsequent accelerator stage with the same on-axis plasma density as the modulator. In this paper we derive the 3D analytic theory for the evolution of the drive pulse in the plasma modulator and show that the spectral modulation is independent of transverse coordinate, which is ideal for compression into a pulse train. We then identify a transverse mode instability (TMI), similar to the TMI observed in optical fiber lasers, which sets limits on the energy of the drive pulse for a given set of laser-plasma parameters. We compare this analytic theory with particle-in-cell (PIC) simulations and find that even higher energy drive pulses can be modulated than those demonstrated in the original proposal.

DOI: [10.1103/PhysRevE.108.015204](https://doi.org/10.1103/PhysRevE.108.015204)**I. INTRODUCTION**

In a laser-plasma accelerator (LPA), plasma oscillations are driven by pushing free electrons away from an ultrashort laser pulse via the ponderomotive force. The heavier ions remain approximately stationary relative to the electrons, thus the electron-ion charge separation collectively forms a strong electric field which can be used to accelerate charged particles. The plasma wave driven in this way will have a phase velocity set by the group velocity of the laser pulse, which is well suited for the acceleration of relativistic charged particles. The accelerating gradients achievable by LPA are set by the wave-breaking field $E_0 = m_e \omega_p c / e$ and can be on the order of 100 GV/m [1], three orders of magnitude larger than those possible in radio-frequency cavities. Here the plasma frequency $\omega_p = (n_e e^2 / m_e \epsilon_0)^{1/2}$, where n_e is the electron density.

Efficient excitation of the plasma wave by a single laser pulse requires that the duration of the pulse is less than half the plasma period $T_p = 2\pi / \omega_p$. For plasma densities of interest T_p is in the 100 fs range, and hence single-pulse LPAs first became practical with the development of chirped pulse

amplification (CPA) [2], which allowed joule-scale pulses to be compressed to sub-picosecond durations. Ever since, most experimental demonstrations of LPAs have used high intensity ultrashort laser pulses from Ti:sapphire CPA laser systems. However, these systems suffer from low (~ 0.1 –10 Hz) repetition rates [3] and poor ($< 0.1\%$) electrical-to-optical energy efficiencies [4]. Despite the advantages gained by being much more compact, the low efficiency and repetition rate of the laser drivers used today severely limit the number of applications for which LPAs offer an advantage over conventional, radio-frequency particle accelerators.

It is important, therefore, to consider alternative laser systems and/or develop novel approaches for driving LPAs. Contemporary thin-disk lasers are efficient and can already provide joule-scale pulses at kHz repetition rates [5–7]. However, they cannot drive a LPA directly since the small bandwidth of their gain media limits the duration of the pulses they generate to [8–10] $\tau \gtrsim 1$ ps, which is much longer than the plasma period. We note that pulses from thin-disk lasers have been compressed to a duration below 100 fs, following spectral broadening via self-phase modulation in a gas [11]. However, to date this approach has been limited to pulse energies below 120 mJ.

With the objective of applying the desirable features of thin-disk lasers to LPAs, some of the present authors recently proposed a scheme, illustrated in Fig. 1, for converting picosecond-duration pulses to a train of shorter pulses that could be used to resonantly excite a plasma wave [12]. In this scheme, which we call the plasma-modulated plasma accelerator (P-MoPA), a high-energy, picosecond-duration

*johannes.vandewetering@physics.ox.ac.uk

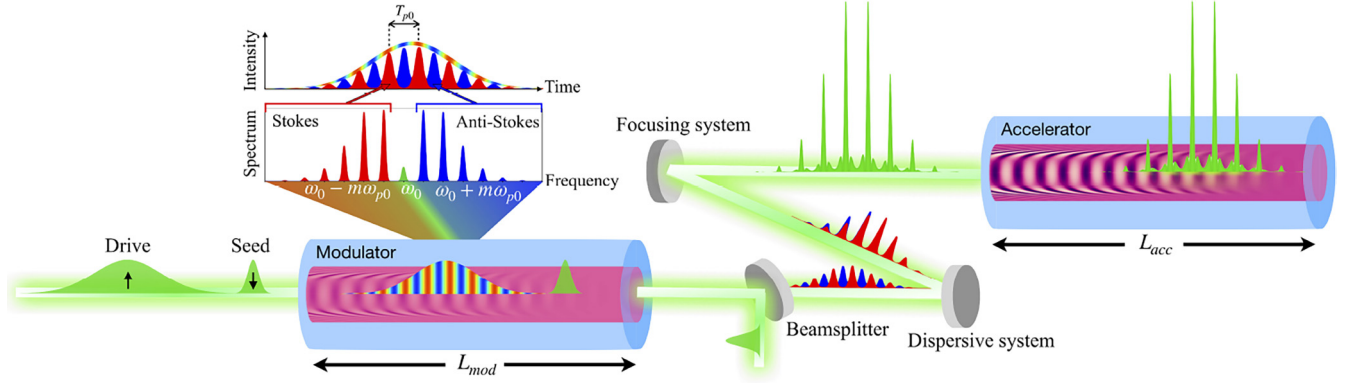


FIG. 1. Outline of the P-MoPA scheme from the original proposal [12]. A short, low-energy seed pulse excites a small wake in the modulator stage which spectrally modulates a long, high-energy drive pulse into interleaving redshifted (Stokes) and blueshifted (anti-Stokes) pulse trains while maintaining a smooth envelope. Chromatic dispersion is then applied to the spectrally modulated drive pulse to compress it into a multipulse train, which can then be used to resonantly drive a wakefield in the accelerator stage with the same density as the modulator.

“drive” pulse is modulated spectrally by copropagating it in a plasma channel with a low amplitude ($\sim 1\%$) plasma wave driven by a low-energy, short “seed” pulse. To first order, the spectral modulation takes the form of a set of sidebands of angular frequencies $\omega_m = \omega_L + m\omega_{p0}$, where ω_L is the angular frequency of the input drive pulse, $m = \pm 1, \pm 2, \pm 3, \dots$ is the sideband order, and ω_{p0} is the plasma frequency on the axis of the plasma channel. The spectrally modulated drive pulse is converted into a temporal modulation by passing it through a dispersive optical system that removes the relative spectral phase, $\psi_m = -|m|\pi/2$, of each sideband. This forms a train of short pulses, spaced temporally by T_{p0} , which can resonantly drive a large amplitude plasma wave in a plasma accelerator stage with the same axial density as the modulator.

In our earlier work a one-dimensional (1D) fluid model, and 2D particle-in-cell (PIC) simulations were used to demonstrate the operation of the plasma modulator and accelerator stages, and to show that GeV-scale energy gains could be obtained from existing thin-disk laser systems. In this paper we derive a full 3D theory of seeded spectral modulation and we use this to establish the useful operating regime for the modulator stage in the P-MoPA. We find that the range of operation of the modulator is determined by the onset of the transverse mode instability (TMI), similar to the TMI observed in high power fiber laser systems [13–17]. This analysis is used to establish the regime of parameter space for which the modulator can be operated successfully. The results of the 3D analytic theory are compared with particle-in-cell (PIC) simulations, and are found to be in good agreement. We find that even higher energy drive pulses can be modulated than those considered in the original proposal.

II. THE PLASMA MODULATOR

A. Seeded spectral modulation in plasma channels

Propagation of the envelope of a laser pulse in an axisymmetric plasma channel of electron density $n_0(r) = n_{00} + \delta n_0(r)$ with a small wake $\delta n(r, \xi; |a|^2)$ can be approximately

described by the paraxial wave equation [18–21] (see Supplemental Material [22] for its derivation)

$$\left[\frac{i}{\omega_L} \frac{\partial}{\partial \tau} + \frac{c^2}{2\omega_L^2} \Delta_{\perp} \right] a = \frac{\omega_p^2}{2\omega_L^2 n_0} [\delta n_0(r) + \delta n(r, \xi; |a|^2) - n_0(r)|a|^2/4] a, \quad (1)$$

where $a(r, \theta, \xi, \tau)$ is the envelope of the pulse’s normalized vector potential with azimuthal angle θ , ω_L is the laser frequency and the propagation is described in comoving coordinates $\xi = z - v_g t$, $\tau = t$, with $v_g/c = (1 - \omega_{p0}^2/\omega_L^2)^{1/2}$ defined as the group velocity of electromagnetic plane waves in uniform plasma of density n_{00} , corresponding to the on-axis plasma channel frequency $\omega_{p0} = \omega_p(r=0)$. This group velocity may differ from the group velocity of a tightly focused laser pulse [23,24]. Nonlinearities come from weakly relativistic effects as well as from interaction between the pulse and its own excited wake.

Successful seeded spectral modulation requires relativistic and self-wake effects to be negligible, which reduces Eq. (1) to a linear paraxial wave equation

$$\left[\frac{i}{\omega_L} \frac{\partial}{\partial \tau} + \frac{c^2}{2\omega_L^2} \Delta_{\perp} \right] a = \frac{\omega_p^2}{2\omega_L^2 n_0} [\delta n_0(r) + \delta n(r, \xi; |a_s|^2)] a, \quad (2)$$

where a_s denotes the seed pulse envelope, whose intensity we assume to be unchanging relative to the modulating drive pulse envelope a . We also demand that the channel is matched to the spot size w_0 of the seed and drive pulses. A matched parabolic channel and its respective unperturbed Gaussian drive pulse envelope take the form [24–26]

$$n_0(r) = n_{00} + \Delta n(r/w_0)^2, \\ a(r, \xi, \tau) = a_0 f(\xi) \exp\left(-\frac{r^2}{w_0^2} - i\omega_L \tau \frac{2c^2}{\omega_L^2 w_0^2}\right), \quad (3)$$

where $\Delta n \equiv (\pi r_e w_0^2)^{-1}$ is the channel depth parameter, r_e is the classical electron radius, and $0 \leq f(\xi) \leq 1$ is the slowly

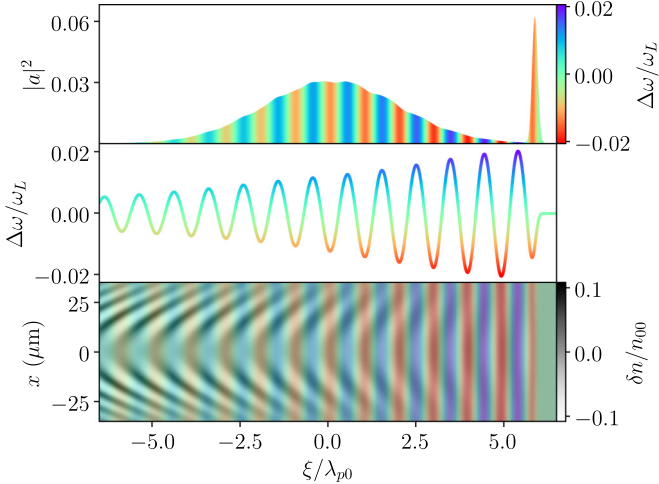


FIG. 2. 2D PIC simulation of the modulator stage in a matched parabolic plasma channel of matched spot size $w_0 = 30 \mu\text{m}$ with $W_{\text{seed}} = 50 \text{ mJ}$ and $W_{\text{drive}} = 0.6 \text{ J}$, $\tau_{\text{drive}} = 1 \text{ ps}$. The top panel shows the on-axis longitudinal intensity profiles $|a|^2$ for the seed and drive pulses. The middle panel plots the on-axis instantaneous frequency calculated by a Hilbert transform. The bottom panel displays the full 2D distributions of the relative amplitude $\delta n/n_0$ of the plasma wave and the relative frequency modulation $\Delta\omega/\omega_L$.

varying longitudinal envelope of the drive pulse. Assuming the seed wake is small relative to the channel depth parameter $|\delta n(r, \xi; |a_s|^2)| \ll \Delta n$, we can apply time-independent perturbation theory to Eq. (2), yielding the following modulation to the total phase of the laser pulse:

$$\Phi(\xi, \tau) = k_L \xi - \frac{2c^2 \tau}{\omega_L w_0^2} \left(1 + \left\langle \frac{\delta n(r, \xi; |a_s|^2)}{\Delta n} \right\rangle_{\perp} \right), \quad (4)$$

where $k_L = \eta \omega_L / c$ is the laser wave number with the on-axis plasma index of refraction $\eta = (1 - \omega_{p0}^2 / \omega_L^2)^{1/2}$ and $\langle (\dots) \rangle_{\perp} = (4/w_0^2) \int_0^{\infty} (\dots) \exp(-2r^2/w_0^2) r dr$ denotes the intensity-weighted transverse average. Using this expression we can also retrieve the shift in instantaneous frequency

$$\frac{\Delta\omega(\xi; L_{\text{mod}})}{\omega_L} = -L_{\text{mod}} \frac{2c^2}{\omega_L^2 w_0^2} \left\langle \frac{\partial}{\partial \xi} \frac{\delta n(r, \xi; |a_s|^2)}{\Delta n} \right\rangle_{\perp}, \quad (5)$$

where $L_{\text{mod}} = v_g \tau$ is the modulator length. This predicts that the spectral modulation amounts to a radial averaging of the longitudinal gradient of the wake weighted by the transverse intensity profile of the drive pulse. This independence of the spectral modulation of radial position is desirable as it allows the spectral modulation to be converted into a temporal one by applying the same chromatic dispersion across the entire cross-section of the modulated pulse. Figure 2 shows the results of a 2D PIC simulation which demonstrates that the spectral modulation is indeed independent of the transverse coordinate, despite the fact that the amplitude and phase of the plasma wave *do* depend on the radial coordinate, as predicted by Eq. (5). This effect can be understood by inspecting the perturbative wake requirement $|\delta n(r, \xi; |a_s|^2)| \ll \Delta n$, from which it follows that the rate of spectral modulation along the modulator must be slow relative to the spot size oscillation frequency [27] $\omega_w = 4c^2/\omega_L w_0^2$. Hence, in this limit,

propagation over many spot size oscillation periods leads to radial averaging of the spectral modulation.

Figure 2 also shows suppression of the spectral modulation towards the tail of the drive pulse, which is most apparent in the plot of the retrieved instantaneous frequency. This is also expected from Eq. (5), since the large curvature of the wavefronts of the plasma wave towards the tail of the drive pulse leads to a reduction in the spectral modulation when the longitudinal gradient of the wave is averaged radially. Note that in the Supplemental Material [22] we compare the results of PIC simulations in 2D and cylindrical geometry. All PIC simulations presented in this paper were performed with axial plasma density $n_{00} = 2.5 \times 10^{17} \text{ cm}^{-3}$, seed and drive laser wavelength $\lambda_L = 1030 \text{ nm}$, seed pulse FWHM duration $\tau_{\text{seed}} = 40 \text{ fs}$, and modulator length $L_{\text{mod}} = 110 \text{ mm}$. A complete list of simulation parameters is included in the Supplemental Material [22].

B. Channel suppression of spectral modulation

As observed in Fig. 2, Eq. (5) implies that the spectral modulation of the drive pulse is limited by wave-front curvature of the plasma wave. For low amplitude wakes this curvature is dominated by the transverse profile of the plasma channel. For square channels the wake has flat phase fronts over most of the transverse profile of the lowest-order mode of the channel. However, for channels with a curved transverse profile, such as parabolic channels, the wave-fronts of the plasma wave are curved, which can strongly suppress the spectral modulation.

Figure 3 shows the results of 2D PIC simulations that compare the performance of a modulator with square and parabolic plasma channels. It can be seen that for the square channel the wave-fronts of the plasma wave are flat across most of the channel width, and as a consequence the pulse train generated by removal of the sideband spectral phase exhibits strong temporal modulation over the entire duration of the pulse train. In contrast, the wave-fronts of the wake driven in a parabolic channel of $30 \mu\text{m}$ matched spot size are strongly curved, and this curvature increases towards the tail of the drive pulse. As a consequence, the generated pulse train does not exhibit complete intensity modulation near its tail, which would reduce the amplitude of the plasma wave it could drive in the accelerator stage. As shown in Fig. 3, increasing the matched spot size of the parabolic channel to $50 \mu\text{m}$ reduces the wake curvature, which leads to improved modulation of the generated pulse train. We note that the deleterious effects of wave-front curvature would be even more pronounced in 3D geometry (see Supplemental Material [22]).

III. STABILITY OF THE PLASMA MODULATOR

It is important to understand the extent to which instabilities will arise in the modulator, and the range of laser and plasma parameters for which any deleterious effects arising from them can be avoided. Since we do not want to waste any of the drive pulse energy within the modulator stage, we would like its envelope to remain smooth as it propagates. Although the specific set of parameters used in the original P-MoPA proposal [12] were shown to work in simulation,

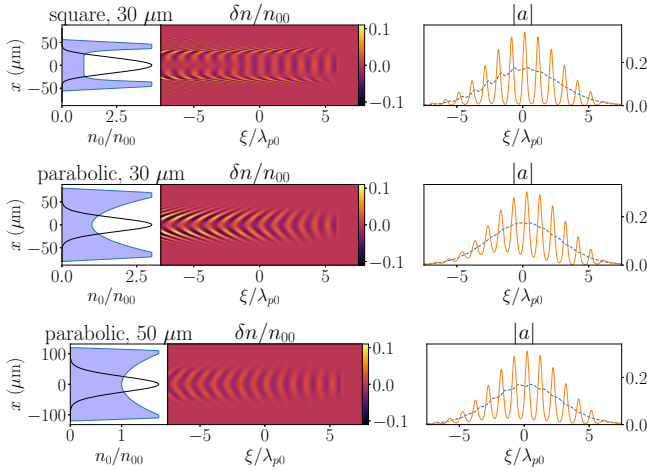


FIG. 3. Comparison of the performance of modulators with plasma channels of different transverse profiles each with wall thicknesses of 20 μm (see Supplemental Material for their parametrizations [22]). The left panels show the transverse electron density (blue) and normalized guided intensity (black) profiles of the channels for: top, a square channel of diameter 30 μm ; middle, a parabolic channel of matched spot size 30 μm ; bottom, a parabolic channel of matched spot size 50 μm (with $(50/30)^2 \times$ more seed and drive pulse energy to account for the larger spot size). The middle panels show the relative wake amplitudes $\delta n/n_{00}$ at the end of the modulator, calculated by 2D PIC simulations. The right panels show the on-axis pulse envelopes $|a|$ at the end of the modulator before (dashed blue) and after (solid orange) the expected [28] sideband spectral phase ψ_m was removed (see Supplemental Material [22]).

for the scheme to be practical we want a large, well-defined parameter space where it is stable.

Increasing the drive pulse energy W_{drive} eventually disrupts the plasma modulator with a TMI via a self-modulation mechanism. This instability drives time-varying wakes which excite higher order transverse channel modes. The results of PIC simulations demonstrating this phenomenon are given in Fig. 4. It can be seen that the Stokes sidebands become more defocused towards the trailing end of the pulse, thereby exciting higher order transverse modes, whereas the

anti-Stokes-shifted light remains relatively well focused. This asymmetry between the Stokes and anti-Stokes light leads to the formation of low-contrast pulse trains in the modulator, with the Stokes-shifted radiation forming a train off-axis, and the anti-Stokes light forming a train on-axis. This effect becomes worse with increasing drive pulse energy, and can be seen to be especially bad for the 2.4 J pulse, which has undergone severe transverse break-up and has been strongly redshifted. This difference in behavior between the Stokes and anti-Stokes sidebands has previously been observed as the result of relativistic effects [29]. As shown in the Supplemental Material [22], a similar effect is predicted in the nonrelativistic regime when nonparaxial effects are accounted for.

A. Envelope self-modulation and raman forward scattering

We now consider the stability of picosecond-scale pulses propagating in long *unperturbed* plasma channels, i.e., in the absence of a wake driven by a seed pulse. As discussed by Mori [30], as long as $1/k_L w_0 \gg \omega_p^2/\omega_L^2$ is satisfied, the following parameter determines whether a laser pulse will be dominated by Raman forward scattering (RFS) or envelope self-modulation (SM) instabilities:

$$\Gamma \equiv \frac{P}{1 \text{ TW}} \frac{\tau_L}{1 \text{ ps}} \left(\frac{n_e}{1 \times 10^{19} \text{ cm}^{-3}} \right)^{5/2} \left(\frac{\lambda_L}{1 \mu\text{m}} \right)^4, \quad (6)$$

where P is the peak laser power and τ_L is the laser duration. When $\Gamma \geq 3$, RFS dominates, whereas SM dominates when $\Gamma \leq 0.4$. Substituting laser-plasma parameters used by Jakobsson *et al.* [12], we find $\Gamma = 6.3 \times 10^{-5}$ and $1/k_L w_0 = 55 \times 10^{-4} \gg \omega_p^2/\omega_L^2 = 2.4 \times 10^{-4}$, meaning that we are well in the SM-dominated regime. The maximum growth rate and e -folding number of envelope SM in a uniform plasma is given by [31,32]

$$\gamma_{\text{SM}} = \frac{1}{8} a_0^2 \frac{\omega_p^2}{\omega_L} (1 + a_0^2)^{-3/2}, \quad N_{e,\text{SM}} = \gamma_{\text{SM}} T_{\text{int}}, \quad (7)$$

where $T_{\text{int}} = L_{\text{mod}}/c$ is the interaction time. The parameters used by Jakobsson *et al.* [12] yield ~ 1.3 e -foldings, and hence SM could become problematic, especially if we try to include more energy in the drive pulse.

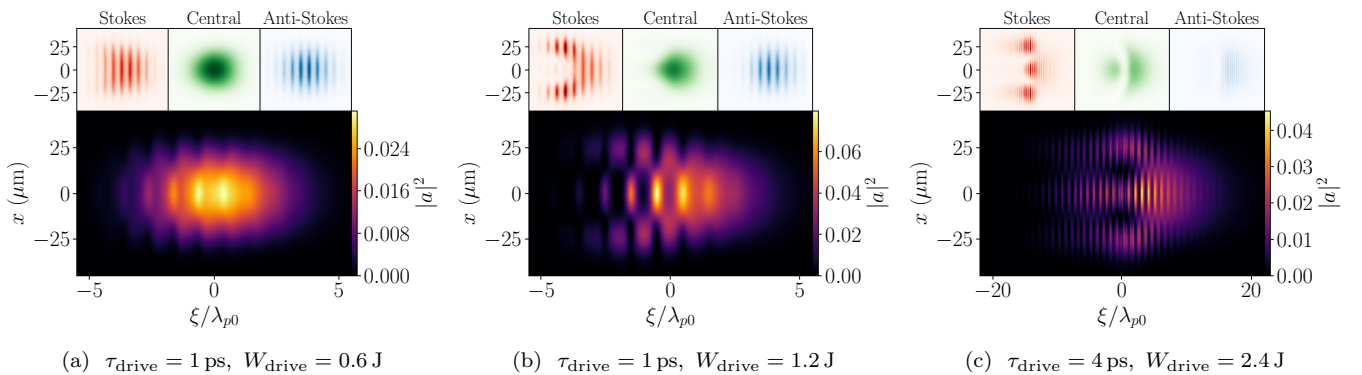


FIG. 4. 2D PIC simulations of the intensity profiles, $|a|^2$, of drive pulses at the exit of the modulator with a channel of square cross-section with $w_0 = 30 \mu\text{m}$ and $W_{\text{seed}} = 50 \text{ mJ}$, for various energies and durations of the drive pulse. The top row displays the intensity profiles decomposed into its redshifted Stokes ($\omega - \omega_L < -\omega_{p0}/2$), central $|\omega - \omega_L| < \omega_{p0}/2$, and blueshifted anti-Stokes ($\omega - \omega_L > \omega_{p0}/2$) components; the bottom panel displays the full intensity profile of the drive pulse.

B. Transverse mode stability condition

For a pulse propagating in a waveguide, the growth of SM is complicated by oscillations in the spot size of the mode, which arise from excitation of more than one waveguide mode. This becomes relevant when the SM growth rate is slower than the spot size oscillation frequency [27] $\gamma_{SM} < \omega_w = 4c^2/\omega_L w_0^2$. In this section we consider the effects of the plasma channel on self-modulation.

Consider coupling a slightly unmatched drive pulse into a parabolic plasma channel so it undergoes small spot size oscillations, and assume that no centroid oscillations are present, so that only radial Laguerre-Gaussian modes $LG_{p0}(r)$ are excited (see Supplemental Material [22]). Neglecting relativistic effects, applying time-dependent perturbation theory to Eq. (1), the coefficients $\alpha_p(\xi, \tau)$ of each radial Laguerre-Gaussian mode p at longitudinal coordinate ξ are found to evolve according to

$$\begin{aligned} \frac{i}{\omega_c} \frac{\partial \alpha_p(\xi, \tau)}{\partial \tau} &= \sum_n \alpha_n(\xi, \tau) \left\langle LG_{p0} \left| \frac{\delta n + \delta n_{NL}}{\Delta n} \right| LG_{n0} \right\rangle \\ &\quad \times e^{i(p-n)\omega_w \tau}, \\ a(r, \xi, \tau) &= e^{-i\omega_c \tau} \sum_p \alpha_p(\xi, \tau) LG_{p0}(r) e^{-ip\omega_w \tau}, \end{aligned} \quad (8)$$

where δn is the fixed seed wake, δn_{NL} is the self-wake of the drive pulse, and ω_w and $\omega_c = \omega_w/2$ are the spot size and centroid oscillation frequencies, respectively [27]. Coupling the drive pulse into a slightly unmatched channel corresponds to the following set of initial conditions,

$$\alpha_0 = a_0 f(\xi), \quad \alpha_1 = \epsilon_w a_0 f(\xi), \quad \alpha_{p \neq 0,1} \approx 0, \quad (9)$$

where $\epsilon_w = -\delta w/w_0 \ll 1$ is the channel spot size mismatch parameter. To solve Eq. (8), the self-wake δn_{NL} must be known. We estimate the self-wake as follows. We first assume that the self-wake can be neglected, and calculate the intensity modulation of the drive pulse caused by the seed wake only. We then use this intensity modulation to calculate the self-wake it would excite. This estimate of the self-wake

$$\begin{aligned} \frac{|a(r, \xi, \tau)|^2}{|a_0|^2 f^2(\xi)} &= \left\{ 1 - 2 \left(\epsilon_w + \frac{\Omega_s \cos(k_{p0}\xi)}{\omega_w} \right) (\cos[\Omega_s \tau \cos(k_{p0}\xi)] - 1) \right\} LG_{00}^2(r) + \left\{ 2\epsilon_w \cos[\Omega_s \tau \cos(k_{p0}\xi)] - \omega_w \tau \right\} \\ &\quad + \frac{2\Omega_s \cos(k_{p0}\xi)}{\omega_w} (\cos[\Omega_s \tau \cos(k_{p0}\xi)] - \omega_w \tau - 1) \left\} LG_{00}(r) LG_{10}(r). \end{aligned} \quad (12)$$

We see from Eq. (12) that the drive pulse is modulated radially, longitudinally, and temporally. This modulation can be physically understood by splitting it into three effects which can be isolated by setting certain terms to zero. The first is a longitudinally uniform spot size oscillation of amplitude δw , which can be recovered by setting $\Omega_s = 0$. The second comes from coupling between the δw spot size oscillations and the seed wake spectral modulation due to the effect mentioned earlier where higher order radial modes spectrally modulate slower than the fundamental mode in the $\sim LG_{00}^2(r)$ seed wake. The third depends purely on the seed wake, which can be seen when setting $\epsilon_w = 0$. The seed wake introduces local

variations in the matched spot size as it perturbs the channel plasma density, varying the spot size longitudinally in ξ and temporally in τ .

To estimate the self-wake δn_{NL} that would be excited by this intensity modulation, we are only interested in keeping terms resonant with the plasma $\sim \cos(k_{p0}\xi + \phi)$ which excite the largest amplitude self-wake. We also only consider propagation times up to $\Omega_s \tau_{mod} \sim 1/2$, as this provides sufficient spectral modulation for compression into a pulse train which roughly coincides with the minimum modulation required to reach the accelerator stage wake amplitude plateau discussed by Jakobsson *et al.* [12]. With both of these considerations in

$$\delta n(r, \xi) = \delta n_s \cos(k_{p0}\xi) LG_{00}^2(r), \quad (10)$$

can then be used to define the plasma modulator stability condition, which sets bounds on the laser-plasma parameters to prevent nonlinear self-modulation from exciting transverse mode transitions.

We will work in the shallow channel limit $\Delta n \ll n_{00}$, which allows us to neglect the effects of the channel on wake structure [33]. This gives a seed wake of the form [18]

$$\begin{aligned} i \frac{\partial \alpha_0}{\partial \tau} &= 2\Omega_s \cos(k_{p0}\xi) \left(\alpha_0 + \frac{1}{2} \alpha_1 e^{-i\omega_w \tau} \right), \\ i \frac{\partial \alpha_1}{\partial \tau} &= 2\Omega_s \cos(k_{p0}\xi) \left(\frac{1}{2} \alpha_0 e^{i\omega_w \tau} + \frac{1}{2} \alpha_1 \right), \end{aligned} \quad (11)$$

where $\Omega_s = (\omega_{p0}^2/8\omega_L)(\delta n_s/n_{00})$ is the rate of spectral modulation parameter. Note that since we are using the paraxial description, we are implicitly assuming symmetry between the Stokes and anti-Stokes sidebands (see Supplemental Material [22] for the nonparaxial description). We can already see from these expressions that the first radial mode spectrally modulates half as fast as the fundamental, as it is more sensitive to the radial drop-off of the seed wake amplitude $\sim LG_{00}^2(r)$. This asymmetry, coupled to spot size oscillations, is one of two effects contributing to plasma-resonant modulations of the drive pulse intensity which excite a self-wake. Since the spot size oscillation frequency is necessarily much higher than the spectral modulation rate, i.e., $\omega_w \gg \Omega_s$, as a consequence of the seed wake being small relative to the channel depth parameter, we can integrate Eq. (11) by assuming most of the light remains in the fundamental mode to find a first order solution $\alpha_0 = \alpha_0^{(0)}(\xi, \tau) + \alpha_0^{(1)}(\xi, \tau)$, $\alpha_1 = \alpha_1^{(1)}(\xi, \tau)$. This yields the following intensity modulation

mind, we can Taylor expand the $\cos[\Omega_s \tau \cos(k_{p0} \xi) - \omega_w \tau]$ terms in Eq. (12) to first order in $\Omega_s \tau$. This gives the

$$|a(r, \xi, \tau)|_{\text{res}}^2 = |a_0|^2 f^2(\xi) \left(2\epsilon_w \Omega_s \tau \sin(\omega_w \tau) + \frac{2\Omega_s [\cos(\omega_w \tau) - 1]}{\omega_w} \right) \cos(k_{p0} \xi) \text{LG}_{00}(r) \text{LG}_{10}(r),$$

$$\frac{\delta n_{\text{NL}}(r, \xi, \tau)}{n_{00}} = \frac{e^2}{8\pi^2 m_e^2 \epsilon_0 c^5} \frac{\omega_{p0} W_{\text{drive}}(\xi) \lambda_L^2}{\pi w_0^2} \left(2\epsilon_w \Omega_s \tau \sin(\omega_w \tau) + \frac{2\Omega_s [\cos(\omega_w \tau) - 1]}{\omega_w} \right) \sin(k_{p0} \xi) \text{LG}_{00}(r) \text{LG}_{10}(r), \quad (13)$$

where $W_{\text{drive}}(\xi)$ indicates the total energy of the drive pulse contained between its head and coordinate ξ . To prevent self-modulation driving transverse mode transitions (and to make this calculation self-consistent), we require that the self-wake effect on the $\text{LG}_{00} \rightarrow \text{LG}_{10}$ transition must be negligible throughout the full propagation in the modulator, resulting in the constraint

$$\int_0^{\tau_{\text{mod}}} \frac{d\tau}{\tau_{\text{mod}}} \langle \text{LG}_{10} | \delta n_{\text{NL}} e^{i\omega_w \tau} | \text{LG}_{00} \rangle \ll \langle \text{LG}_{10} | \delta n | \text{LG}_{00} \rangle. \quad (14)$$

Substituting $\Omega_s \tau_{\text{mod}} = 1/2$ and Eq. (13) into this constraint yields the plasma modulator transverse mode stability condition

$$\left| \frac{\delta w/w_0}{\delta n_s/n_{00}} + \frac{k_{p0}^2 w_0^2}{8} \right| \frac{\omega_{p0} W_{\text{drive}} \lambda_L^2}{\pi w_0^2} \ll P_{\text{mod}},$$

$$P_{\text{mod}} = \frac{32\pi^2 m_e^2 \epsilon_0 c^5}{e^2} \approx 220 \text{ GW}. \quad (15)$$

This sets a limit on the total energy of the drive pulse W_{drive} for a given plasma density, spot size, laser wavelength, seed wake and channel spot size mismatch. For the laser-plasma parameters used by Jakobsson *et al.* [12], taking $\delta n_s/n_{00} \sim 2.5\%$ and $\delta w/w_0 \sim 12\%$ from the PIC simulations therein, the requirement of Eq. (15) becomes $37 \text{ GW} \ll 220 \text{ GW}$, which is satisfied. Hence, in this regime we do not expect the self-modulation effects to be debilitating to the plasma modulator. In PIC simulations, we have found that even letting the LHS of Eq. (15) go up to $\sim 70 \text{ GW}$ remains stable enough for compression into a pulse train despite the excitation of the first radial mode being nonnegligible. Figure 5 shows the calculated intensity profiles, $|a|^2$, of drive pulses at the exit of the modulator before and after compression into a pulse train (by removing the expected [28] sideband spectral phase ψ_m of a pulse without TMI (see Supplemental Material [22])) for drive pulses of energy $W_{\text{drive}} = 1.2 \text{ J}$ and various pulse durations. It can be seen that, despite the pulse duration varying by a factor of 16, they each undergo the same amount of spot size oscillation driven transitions to higher order transverse modes. This is in agreement with Eq. (15), which is independent of the drive pulse duration. As a consequence, for drive pulses of duration 1, 2 and 4 ps, the transverse structure of the pulse at the end of the modulator is identical. For drive pulses of 250 fs duration, the structure is also similar, but in this case the pulse duration is only approximately two plasma periods long, and hence the assumption of small bandwidth breaks down. We note also that Fig. 5 shows that in each case the spectrally modulated drive pulse can still be compressed

into a well-defined pulse train suitable for the accelerator stage, despite the transverse structure that it has developed.

For most practical applications, the spot size oscillations will be determined by the mismatch between the transverse amplitude profile of the lowest-order channel mode, and that of the drive pulse at the channel entrance. However, even in the limit of a perfectly matched channel, small spot size oscillations can arise from other sources, such as ponderomotive and relativistic self-focusing [35,36]. In addition, the $k_{p0}^2 w_0^2/8$ term in Eq. (15), which comes from the seed wake forming a plasma-resonant variation in matched spot size, ensures that there will always be an upper limit on the drive pulse energy.

There are two ways that excitation of higher order transverse modes can be mitigated, other than ensuring that Eq. (15) is satisfied. However, each of these comes at a cost. First, the treatment above assumed propagation in a shallow channel. For deeper channels, i.e. $\Delta n \sim n_{00}$, the

excitation of higher order transverse modes can be mitigated, other than ensuring that Eq. (15) is satisfied. However, each of these comes at a cost. First, the treatment above assumed propagation in a shallow channel. For deeper channels, i.e. $\Delta n \sim n_{00}$, the

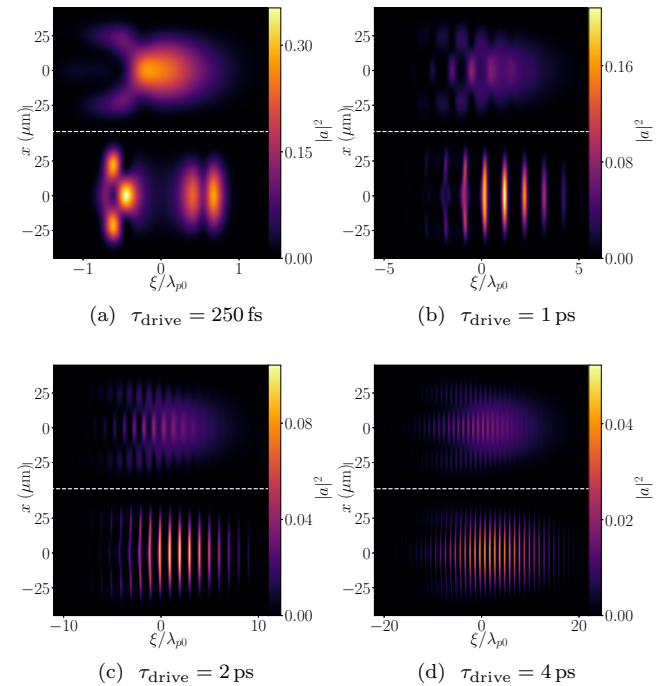


FIG. 5. Calculated intensity profiles, $|a|^2$, of drive pulses at the exit of the modulator before (top) and after (bottom) compression into a pulse train for drive pulses of energy $W_{\text{drive}} = 1.2 \text{ J}$ and FWHM duration: (a) 0.25 ps, (b) 1 ps, (c) 2 ps, and (d) 4 ps. For these 2D PIC simulations the modulator was taken to have a square cross-section with $w_0 = 30 \mu\text{m}$, and the seed pulse to have an energy of $W_{\text{seed}} = 50 \text{ mJ}$.

self-wake will be partially suppressed by the off-resonant plasma wave, and the difference in spectral modulation rate of the higher-order mode and the fundamental will be decreased due to the radial component of the seed wake. This allows for more energy to propagate in the modulator without transitions to higher order modes. However, channels of this form also suppress the spectral modulation towards the tail of the pulse, as shown in Fig. 3, which is detrimental to pulse compression. Another option would be to use a leaky channel that leaks higher order modes faster than the fundamental mode [37,38]. However, this approach would have reduced efficiency, since drive pulse energy transferred to higher order modes would be lost.

IV. CONCLUSION

We have derived a full 3D analytic theory of seeded spectral modulation, and have used this to establish the useful operating regime for the modulator stage in the P-MoPA. This model is found to be in very good agreement with those obtained from 2D PIC simulations of the modulator.

The analytic theory leads to several important conclusions. First, the spectral modulation of the drive pulse is independent of radial distance from the axis of the modulator channel. This ensures that, after leaving the modulator, the entire spectrally modulated pulse can be compressed by a simple optical system that removes the spectral phase accumulated in the modulator. Second, curvature of the seed-pulse-driven plasma waves is shown to reduce the degree of spectral modulation, and hence the modulation of the pulse train that is generated after compression. This finding establishes limits on the shape of the channel used in a P-MoPA modulator.

We also explored limits to the operating parameters of a seeded modulator set by the self-modulation of the drive pulse and excitation of higher-order transverse channel modes. We found that the operation of the modulator is limited by the onset of the transverse mode instability (TMI), similar to the TMI observed in high power fiber laser systems. An analysis of the excitation of higher-order modes allowed the identification of a condition on the energy of the drive pulse, the relative amplitude of oscillations in its spot size, and the relative amplitude of the seed-pulse-driven wake, that must be satisfied for stable operation.

In this work we considered plasma channels with parabolic and square profiles to examine the behavior of the modulator

for two possible extremes: deep parabolic channels introduce strong wake phase-front curvature, whilst square channels maintain completely flat wake phase-fronts up to their walls. In laboratory settings, the long ($\gtrsim 100$ mm), low-attenuation plasma channels required for this scheme can be generated by the conditioned hydrodynamic optical-field-ionized (CHOFI) technique [39–41], which forms deep, low-loss channels with on-axis densities as low as 1×10^{17} cm⁻³. Furthermore, CHOFI channels have been demonstrated to be operable at kHz repetition rates [42], which is ideal for the P-MoPA scheme, and recently resonant excitation of a plasma wakefield by a train of pulses guided in a 110-mm-long CHOFI channel has been demonstrated [43]. These CHOFI plasma channels will have a transverse profile somewhere between the two extreme cases considered in the present paper. Hence, some wake phase-front curvature is expected for CHOFI channels, but this will be less pronounced than for a parabolic channel.

Finally, we emphasize that the results presented here show that the modulator in a P-MoPA can exhibit stable operation over a much broader range of operating parameters than considered in the original proposal [12]. This includes operation at higher drive pulse energies, which bodes well for the development of high-repetition-rate, GeV-scale P-MoPAs.

ACKNOWLEDGMENTS

This work was supported by the UK Engineering and Physical Sciences Research Council (EPSRC) (Grant No. EP/V006797/1), the UK Science and Technologies Facilities Council (Grant No. ST/V001655/1), InnovateUK (Grant No. 10059294), United Kingdom Research and Innovation (UKRI) ARCHER2 Pioneer Projects (Grant No. ARCHER2 PR17125) [44], and the Ken and Veronica Tregidgo Scholarship in Atomic and Laser Physics. This publication arises from research funded by the John Fell Oxford University Press Research Fund. This research used the open-source particle-in-cell code WarpX [45,46], primarily funded by the US DOE Exascale Computing Project. Primary WarpX contributors are with LBNL, LLNL, CEA-LIDYL, SLAC, DESY, CERN, and Modern Electron. We acknowledge all WarpX contributors. This research was funded in whole, or in part, by EPSRC and STFC, which are Plan S funders. The input decks used for the PIC simulations presented in this paper are available at Ref. [47].

-
- [1] T. Tajima and J. M. Dawson, Laser Electron Accelerator, *Phys. Rev. Lett.* **43**, 267 (1979).
 - [2] D. Strickland and G. Mourou, Compression of amplified chirped optical pulses, *Opt. Commun.* **56**, 219 (1985).
 - [3] J. W. Dawson, J. K. Crane, M. J. MESSERLY, M. A. Prantil, P. H. Pax, A. K. Sridharan, G. S. Allen, D. R. Drachenberg, H. H. Phan, J. E. Heebner, C. A. Ebberts, R. J. Beach, E. P. Hartouni, C. W. Siders, T. M. Spinka, C. P. J. Barty, A. J. Bayramian, L. C. Haefner, F. Albert, W. H. Lowdermilk *et al.*, High average power lasers for future particle accelerators, *AIP Conf. Proc.* **1507**, 147 (2012).
 - [4] B. Hidding, S. Hooker, S. Jamison, B. Muratori, C. Murphy, Z. Najmudin, R. Pattathil, G. Sarri, M. Streeter, C. Welsch, M. Wing, and G. Xia, Plasma wakefield accelerator research 2019–2040: A community-driven UK roadmap compiled by the plasma wakefield accelerator steering committee (PWASC), [arXiv:1904.09205](https://arxiv.org/abs/1904.09205).
 - [5] C. Herkommer, P. Krötz, R. Jung, S. Klingebiel, C. Wandt, R. Bessing, P. Walch, T. Produit, K. Michel, D. Bauer, R. Kienberger, and T. Metzger, Ultrafast thin-disk multipass amplifier with 720 mJ operating at kilohertz repetition rate for applications in atmospheric research, *Opt. Express* **28**, 30164 (2020).

- [6] S. Nagel, B. Metzger, D. Bauer, J. Dominik, T. Gottwald, V. Kuhn, A. Killi, T. Dekorsy, and S.-S. Schad, Thin-disk laser system operating above 10 kW at near fundamental mode beam quality, *Opt. Lett.* **46**, 965 (2021).
- [7] T. Produit, P. Walch, C. Herkommer, A. Mostajabi, M. Moret, U. Andral, A. Sunjerga, M. Azadifar, Y.-B. André, B. Mahieu, W. Haas, B. Esmiller, G. Fournier, P. Krötz, T. Metzger, K. Michel, A. Mysyrowicz, M. Rubinstein, F. Rachidi, J. Kasparian *et al.*, The laser lightning rod project, *Eur. Phys. J. Appl. Phys.* **93**, 10504 (2021).
- [8] R. Paschotta, J. Aus der Au, G. Spühler, S. Erhard, A. Giesen, and U. Keller, Passive mode locking of thin-disk lasers: Effects of spatial hole burning, *Appl. Phys. B* **72**, 267 (2001).
- [9] T. Südmeier, C. Kränkel, C. Baer, O. Heckl, C. Saraceno, M. Golling, R. Peters, K. Petermann, G. Huber, and U. Keller, High-power ultrafast thin disk laser oscillators and their potential for sub-100-femtosecond pulse generation, *Appl. Phys. B* **97**, 281 (2009).
- [10] C. R. E. Baer, C. Kränkel, C. J. Saraceno, O. H. Heckl, M. Golling, R. Peters, K. Petermann, T. Südmeier, G. Huber, and U. Keller, Femtosecond thin-disk laser with 141 W of average power, *Opt. Lett.* **35**, 2302 (2010).
- [11] M. Kaumanns, D. Kormin, T. Nubbemeyer, V. Pervak, and S. Karsch, Spectral broadening of 112 mJ, 1.3 ps pulses at 5 kHz in a LG₁₀ multipass cell with compressibility to 37 fs, *Opt. Lett.* **46**, 929 (2021).
- [12] O. Jakobsson, S. M. Hooker, and R. Walczak, GeV-scale Accelerators Driven by Plasma-Modulated Pulses from Kilohertz Lasers, *Phys. Rev. Lett.* **127**, 184801 (2021).
- [13] T. Eidam, S. Hanf, E. Seise, T. V. Andersen, T. Gabler, C. Wirth, T. Schreiber, J. Limpert, and A. Tünnermann, Femtosecond fiber CPA system emitting 830 W average output power, *Opt. Lett.* **35**, 94 (2010).
- [14] T. Eidam, C. Wirth, C. Jauregui, F. Stutzki, F. Jansen, H.-J. Otto, O. Schmidt, T. Schreiber, J. Limpert, and A. Tünnermann, Experimental observations of the threshold-like onset of mode instabilities in high power fiber amplifiers, *Opt. Express* **19**, 13218 (2011).
- [15] C. Jauregui, T. Eidam, J. Limpert, and A. Tünnermann, Impact of modal interference on the beam quality of high-power fiber amplifiers, *Opt. Express* **19**, 3258 (2011).
- [16] A. V. Smith and J. J. Smith, Mode instability in high power fiber amplifiers, *Opt. Express* **19**, 10180 (2011).
- [17] C. Jauregui, C. Stihler, and J. Limpert, Transverse mode instability, *Adv. Opt. Photon.* **12**, 429 (2020).
- [18] E. Esarey, P. Sprangle, J. Krall, A. Ting, and G. Joyce, Optically guided laser wake-field acceleration*, *Phys. Fluids B: Plasma Phys.* **5**, 2690 (1993).
- [19] N. E. Andreev, L. M. Gorbunov, V. I. Kirsanov, A. A. Pogosova, and R. R. Ramazashvili, The theory of laser self-resonant wake field excitation, *Phys. Scr.* **49**, 101 (1994).
- [20] P. Mora and T. M. Antonsen, Jr., Kinetic modeling of intense, short laser pulses propagating in tenuous plasmas, *Phys. Plasmas* **4**, 217 (1997).
- [21] W. Zhu, J. P. Palastro, and T. M. Antonsen, Studies of spectral modification and limitations of the modified paraxial equation in laser wakefield simulations, *Phys. Plasmas* **19**, 033105 (2012).
- [22] See Supplemental Material at <http://link.aps.org/supplemental/10.1103/PhysRevE.108.015204> for further details on the theory and particle-in-cell simulations presented, which includes Refs. [12,23,24,33,44].
- [23] E. Esarey, P. Sprangle, M. Pilloff, and J. Krall, Theory and group velocity of ultrashort, tightly focused laser pulses, *J. Opt. Soc. Am. B* **12**, 1695 (1995).
- [24] E. Esarey and W. P. Leemans, Nonparaxial propagation of ultrashort laser pulses in plasma channels, *Phys. Rev. E* **59**, 1082 (1999).
- [25] C. Kurtz and W. Streifer, Guided waves in inhomogeneous focusing media part I: Formulation, solution for quadratic inhomogeneity, *IEEE Trans. Microwave Theory Tech.* **17**, 11 (1969).
- [26] W. Firth, Propagation of laser beams through inhomogeneous media, *Opt. Commun.* **22**, 226 (1977).
- [27] A. J. Gonsalves, K. Nakamura, C. Lin, J. Osterhoff, S. Shiraishi, C. B. Schroeder, C. G. R. Geddes, C. Tóth, E. Esarey, and W. P. Leemans, Plasma channel diagnostic based on laser centroid oscillations, *Phys. Plasmas* **17**, 056706 (2010).
- [28] For Supplemental Material see Ref. [12].
- [29] P. Gibbon, The self-trapping of light waves by beat-wave excitation, *Phys. Fluids B: Plasma Phys.* **2**, 2196 (1990).
- [30] W. Mori, The physics of the nonlinear optics of plasmas at relativistic intensities for short-pulse lasers, *IEEE J. Quant. Electron.* **33**, 1942 (1997).
- [31] C. E. Max, J. Arons, and A. B. Langdon, Self-Modulation and Self-Focusing of Electromagnetic Waves in Plasmas, *Phys. Rev. Lett.* **33**, 209 (1974).
- [32] E. Esarey, P. Sprangle, J. Krall, and A. Ting, Self-focusing and guiding of short laser pulses in ionizing gases and plasmas, *IEEE J. Quant. Electron.* **33**, 1879 (1997).
- [33] N. E. Andreev, L. M. Gorbunov, V. I. Kirsanov, K. Nakajima, and A. Ogata, Structure of the wake field in plasma channels, *Phys. Plasmas* **4**, 1145 (1997).
- [34] M. N. Rosenbluth and C. S. Liu, Excitation of Plasma Waves by Two Laser Beams, *Phys. Rev. Lett.* **29**, 701 (1972).
- [35] M. Siegrist, Self-focusing in a plasma due to ponderomotive forces and relativistic effects, *Opt. Commun.* **16**, 402 (1976).
- [36] H. S. Brandi, C. Manus, G. Mainfray, T. Lehner, and G. Bonnaud, Relativistic and ponderomotive self-focusing of a laser beam in a radially inhomogeneous plasma. I. Paraxial approximation, *Phys. Fluids B: Plasma Phys.* **5**, 3539 (1993).
- [37] B. Z. Djordjević, C. Benedetti, C. B. Schroeder, E. Esarey, and W. P. Leemans, Laser mode control using leaky plasma channels, *AIP Conf. Proc.* **1812**, 040013 (2017).
- [38] B. Z. Djordjević, C. Benedetti, C. B. Schroeder, E. Esarey, and W. P. Leemans, Filtering higher-order laser modes using leaky plasma channels, *Phys. Plasmas* **25**, 013103 (2018).
- [39] A. Picksley, A. Alejo, R. J. Shalloo, C. Arran, A. von Boetticher, L. Corner, J. A. Holloway, J. Jonnerby, O. Jakobsson, C. Thornton, R. Walczak, and S. M. Hooker, Meter-scale conditioned hydrodynamic optical-field-ionized plasma channels, *Phys. Rev. E* **102**, 053201 (2020).
- [40] L. Feder, B. Miao, J. E. Shrock, A. Goffin, and H. M. Milchberg, Self-waveguiding of relativistic laser pulses in neutral gas channels, *Phys. Rev. Res.* **2**, 043173 (2020).
- [41] B. Miao, L. Feder, J. E. Shrock, A. Goffin, and H. M. Milchberg, Optical Guiding in Meter-Scale Plasma Waveguides, *Phys. Rev. Lett.* **125**, 074801 (2020).

- [42] A. Alejo, J. Cowley, A. Picksley, R. Walczak, and S. M. Hooker, Demonstration of kilohertz operation of hydrodynamic optical-field-ionized plasma channels, *Phys. Rev. Accel. Beams* **25**, 011301 (2022).
- [43] A. Ross, E. Archer, N. Bourgeois, J. Chappell, J. Cowley, L. Feder, O. Jakobsson, H. Jones, A. Picksley, L. Reid, J. J. van de Wetering, W.-T. Wang, L. Corner, R. Walczak, and S. M. Hooker, Observation of resonant wakefield excitation by pulse trains guided in long plasma channels, in *Proceedings of the 20th Advanced Accelerator Concepts Workshop* (Long Island, NY, 2022).
- [44] <https://www.archer2.ac.uk>.
- [45] L. Fedeli, A. Huebl, F. Boillod-Cerneux, T. Clark, K. Gott, C. Hillairet, S. Jaure, A. Leblanc, R. Lehe, A. Myers, C. Piechurski, M. Sato, N. Zaim, W. Zhang, J. Vay, and H. Vincenti, Pushing the frontier in the design of laser-based electron accelerators with groundbreaking mesh-refined particle-in-cell simulations on exascale-class supercomputers, in *Proceedings of the International Conference for High Performance Computing, Networking, Storage and Analysis (SC'22)* (IEEE Computer Society, Los Alamitos, CA, 2022), pp. 25–36.
- [46] <https://github.com/ECP-WarpX/WarpX>.
- [47] <http://doi.org/10.5281/zenodo.7734261>.